Thermal analysis of turbulent Poiseuille flows

Felipe J. O. Ribeiro
feliperibeiro.ufu@gmail.com
Av. João Naves de Ávila, 2121, Campos Santa Mônica, Uberlândia, MG

Aristeu da Silveira Neto
aristeus@ufu.br
Av. João Naves de Ávila, 2121, Campos Santa Mônica, Uberlândia, MG

July 12, 2020

Abstract

On the present paper the authors develop a semi-exact meta-modeled approach for thermal analysis on turbulent Poiseuille flows with a detailed study concerning the impact of different and innovative parameterizations of the turbulent Prandtl number and the Cebeci constant. The physical model consisted on a plan channel with isothermal walls that varies linearly in temperature on the stream-wise direction, resulting in an statistical permanent regime for the temperature and velocity profiles. The parametrization of the turbulent Prandtl number and the Cebeci's constant were modified aiming to achieve better accuracy when compared with the DNS solution. For the development of new models for these constants, genetic algorithms were used resulting in new functions capable of describing the turbulent Prandtl number and the Cebeci's constant for this specific problem. According to the numerical results, these new models concerning the Turbulent Prandtl number and the Cebeci's constant are capable of substantially increase the accuracy of the semi-exact method. Finally, the generally accepted classical models for these constants failed to properly represent the turbulent Poiseuille flow, what resulted in inaccuracy, this was corrected by the new models from the present research.

Keywords - Turbulent Prandtl number, Cebeci's constant, Turbulent Poiseuille flow, Genetic algorithm, DNS.

1 Introduction

It is well known that the field of turbulent fluid dynamics is capable of such high complexity that, even nowadays, it is not completely understood, as described by O. Basim and Hasan, 2007 [1]. Out of the domain of Direct Numerical Simulations (DNS), all sorts of approximations have to be assumed to properly mathematically develop the Navier-Stokes equations. The nonlinear nature of these systems [2] make difficult for a continuous mathematical solution.

Despite the difficulty, a big part of the scientific community is studying turbulence on fluid and thermal dynamics. There is a great interest from the industry and academia because of opportunities for great machinery optimization and the study of chaotic dynamic behavior.

As turbulence results in a nonlinear dynamic system, it is impossible to determine an algebraic solution for most cases. Them, the numerical approach is done, with the discretization of space and time. Solving such linear systems requires enormous computational power since the number of elements required to properly simulate the phenomenon is very big. RANS, URANS and LES are alternatives. They consists in not numerically resolving the Naiver-Stokes equation on all scales required, but instead substituting some tensors and other nonlinear therms by conceptual and experimental approximations.

Such methods are important because they offer a much quicker solution. The DNS (Direct Numerical Solution) approach demands high computational work, as it considers all scales of complexity, not even being possible or viable in some cases [6], as explained on H. Kawamura, H. Abe and Yuichi Matsuo's work [7]. But, in the other hand, these approximated methods result in mathematical inaccuracies.

On the present paper, the authors aim to develop a semi analytical RANS (Reynold's Averaged Navier-Stokes) method with the averaged energy equation to describe the thermal configuration on turbulent plan Poiseuille flows [8], modeled with the mixture length methodology by Ludwig Prandtl. It relies on the Boussinesq hypothesis for being a way of modeling the Reynolds shear tensor and to close the filtered Navier-Stokes and energy equations. In this context, some parameters that worth mentioning are the turbulent Prandtl number [3] and the constant $A = 26$, on Cebeci's damping formulation [4]. These parameters are used for modeling important properties of the fluid's thermal diffusion and dynamics as exposed by Silveira-Neto, 2018 [5]. Meta-models were developed for the turbulent Prandtl number and the Cebeci's constant with a genetic algorithm to enhance the results compared to DNS solutions. Such implementation resulted on accuracy and efficiency giving birth to new models for these parameters. The results of this work's formulation were compared with the DNS ([9] , [10]) aiming to provide a detailed analysis on the viability of meta models on Poiseuille turbulent flows with thermal effects.

2 Physical model

The problem was defined as a plan channel flow, with only one finite dimension on the y axis. Two boundary walls were set at perpendicular plans to the y axis, as nonslip infinite plates and in a constant thermal flux regime. The z axis was proposed self similar both on velocity and temperature, resulting on a plan domain (Fig.1). The flow was considered incompressible and the fluid was considered Newtonian. The fluid flows, in average, on the x axis direction. The Reynolds numbers $Re = \frac{2R\overline{U}}{\nu}$ ranges from 4560 to 41441, resulting on a turbulent regime.

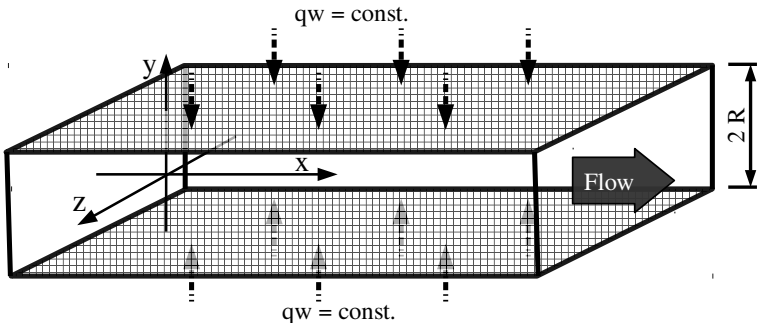

Figure 1: Geometric definition and boundary condition of the system.

The mathematical formulation for the problem was based on the continuity and Navier-Stokes equations, as presented on Cengel's book [11], and the thermal energy transport equation, as presented on Freank's Incropera [12]. These were the assumptions made to the proposed problem, that will be considered on the differential mathematical model ahead.

3 Differential mathematical model

The mean continuity (Eq.1), the mean Navier-Stokes (Eq.2) and the mean thermal energy (Eq.3) equations are presented as follows:

$$\frac{\partial \overline{u}}{\partial x} = 0, \tag{1}$$

$$\frac{\partial \overline{u}\,\overline{v}}{\partial y} = -\frac{1}{\rho}\frac{\partial \overline{p}}{\partial x} + \frac{\partial}{\partial y}\left(\nu\frac{\partial \overline{u}}{\partial y} - \overline{u'v'}\right), \tag{2}$$

$$\frac{\partial}{\partial x}\left(\overline{T'u'}\right) + \frac{\partial}{\partial x}\left(\overline{u}\overline{T}\right) + \frac{\partial}{\partial y}\left(\overline{T'v'}\right) + \frac{\partial}{\partial y}\left(\overline{v}\overline{T}\right) = \frac{\partial}{\partial x}\left(\alpha\frac{\partial \overline{T}}{\partial x}\right) + \frac{\partial}{\partial y}\left(\alpha\frac{\partial \overline{T}}{\partial y}\right). \tag{3}$$

Being $\overline{u}$ and $\overline{v}$ the mean velocities and u' and v' the velocities´s fluctuations in x and y directions, ρ the specific mass, $\overline{p}$ the mean pressure, ν the kinematic viscosity, $\overline{T}$ the mean temperature, T' the temperature fluctuation and α the thermal diffusivity.

The time independence and mean characterization of the system define the method as an Averaged Navier Stokes (RANS) methodology.

3.1 The temperature permanent regime

The velocity field is completely developed on the channel, for mean values (Fig. 3), but this is not the case for the temperature field, as a constant thermal flux is imposed over the walls. The temperature keeps increasing in the domain, never settling down.
Even considering the mean values, the temperature field of a turbulent channel flow don't converge naturally to a unidimensional permanent state (Fig. 2).

In a effort to simplify the solution, the thermal configuration was studied with a thermal energy balance (Eq. 4).

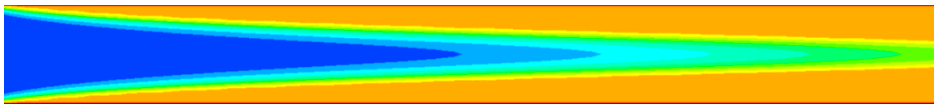

Figure 2: Temperature field not in statistical permanent regime inside a channel. Profile constant in the XY plan.

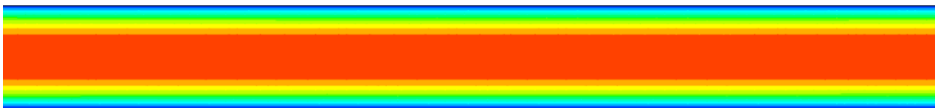

Figure 3: Velocity field in statistical permanent regime inside a channel. Profile constant in the XY plan.

$$q_{conv.} = \dot{m} C_p \Delta T_m, \tag{4}$$

Where $q_{conv.}$ is the heat from convection, $\dot{m}$ the mass flux, C_p the specific heat capacity and T_m is the average temperature in a cross-section.

$$2 q_w b \Delta x = \dot{m} C_p \Delta T_m, \tag{5}$$

Where b is the depth of the channel and q_w is the heat from walls. So, substituting $\dot{m} = u_m 2Rb\rho$, where u_m is the medium velocity in the channel's cross section and R the channel half width(Fig.1), and assuming $\Delta T_m = \frac{\partial(\overline{T}_m)}{\partial x}\Delta x$:

$$2 q_w b \Delta x = u_m 2Rb\rho C_p \frac{\partial\left(\overline{T}_m\right)}{\partial x}\Delta x, \tag{6}$$

$$q_w = u_m R\rho C_p \frac{\partial\left(\overline{T}_m\right)}{\partial x}, \tag{7}$$

$$\frac{\partial\left(\overline{T}_m\right)}{\partial x} = \frac{q_w}{u_m R\rho C_p}. \tag{8}$$

As all therms on the right side are constants, so the mean temperature had to varies linearly on the stream-wise direction. To better understand the wall temperature with such energy profile, a convective thermal formulation was used, which can be expressed mathematically by:

$$q_w = hA\left(T_w(x) - \overline{T}_m(x)\right). \tag{9}$$

It should be observed that the h value is a constant since this is a fully dynamically developed flow. Thus, using Eq. 8, it is possible to write:

$$\frac{dT_w(x)}{dx} = \frac{d\overline{T}_m(x)}{dx} = Cte. \tag{10}$$

With the temperature on the walls and the mean temperature gradient set as linear by these mathematical statements, it was possible to extend this gradient to all the domain considering the boundary conditions and the symmetry of the system. So a constant temperature gradient was imposed on the heated walls creating a boundary condition of constant thermal flux, resulting on all the temperature field to varies linearly on the x axis and with time. The temperature value was then decomposed to the form $T^*(y) = T(x,y) - T_w(x)$ where $T_w(x)$ is the temperature at the wall, resulting in a similarity effect on the streamwise direction, resuming the problem to a unidimensional representative state for the variable $T^*(y)$. Therefore, this decomposition was replaced in Eq. 3:

$$\begin{aligned}\frac{\partial}{\partial x}\left(\overline{(T^* + T_w)'u'}\right) + \frac{\partial}{\partial x}\left(\overline{(T^* + T_w)}\overline{u}\right) + \frac{\partial}{\partial y}\left(\overline{(T^* + T_w)'v'}\right) + \frac{\partial}{\partial y}\left(\overline{(T^* + T_w)}\overline{v}\right) = \\ \frac{\partial}{\partial x}\left(\alpha\frac{\partial\overline{(T^* + T_w)}}{\partial x}\right) + \frac{\partial}{\partial y}\left(\alpha\frac{\partial\overline{(T^* + T_w)}}{\partial y}\right).\end{aligned} \tag{11}$$

Then the expression could be further developed algebraically considering all mean velocity on y and z axis null:

$$\frac{\partial}{\partial y}\left(\alpha\frac{\partial\overline{T^*}}{\partial y} - \left(\overline{T^{*\prime}v'}\right)\right) = \overline{u}\frac{\partial\overline{T_w}}{\partial x}. \tag{12}$$

3.2 The Boussinesq hypothesis

Now, on a unidimensional simplified expression, the model requires a closure model for the turbulent flux of thermal energy. So the Boussinesq hypothesis was used. The term $\overline{T^{*\prime}v^{\prime}}$ can be modeled with:

$$-\left(\overline{T^{*\prime}v^{\prime}}\right) = \alpha_t \frac{\partial \overline{T^*}}{\partial y}. \tag{13}$$

Where α_t is the turbulent thermal diffusivity. The following equation can be obtained by substituting (13) in the main equation (12):

$$\frac{\partial}{\partial y}\left[(\alpha + \alpha_t)\frac{\partial \overline{T^*}}{\partial y}\right] = \overline{u}\frac{\partial \overline{T_w}}{\partial x}. \tag{14}$$

3.3 Prandtl mixing length model

The term of the turbulent thermal diffusion, α_t, needs to be modeled. The classical concept of the turbulent Prandtl number is used in the present work:

$$Pr_t = \frac{\nu_t}{\alpha_t}. \tag{15}$$

The turbulent kinematic viscosity ν_t need to be modeled. The value of the turbulent Prandtl number $Pr_t = 0.71$ has been used in the literature. With the Prandtl mixing length model, it is defined:

$$\nu_t = l_m^2 \left|\frac{\partial \overline{u}}{\partial y}\right|. \tag{16}$$

$$\alpha_t = \frac{l_m^2}{Pr_t}\left|\frac{\partial \overline{u}}{\partial y}\right|. \tag{17}$$

Where l_m is the mixing length. Then, substituting (17) in (14):

$$\frac{\partial}{\partial y}\left(\left(\alpha + \frac{l_m^2\left|\frac{\partial \overline{u}}{\partial y}\right|}{Pr_t}\right)\frac{\partial \overline{T^*}}{\partial y}\right) = \overline{u}\frac{\partial}{\partial x}\left(\overline{T_w}\right). \tag{18}$$

It is possible to notice, when analyzing the dynamics of the flow, that for positive values of y, see figure 1, the first derivative of velocity will always be negative, since we have a velocity that decreases with the increase of y. It results in:

$$\frac{\partial}{\partial y}\left(\left(\alpha - \frac{l_m^2}{Pr_t}\frac{\partial \overline{u}}{\partial y}\right)\frac{\partial \overline{T^*}}{\partial y}\right) = \overline{u}\frac{\partial}{\partial x}\left(\overline{T_w}\right). \tag{19}$$

3.4 The mixing length

The mixing length l_m needs to be modeled. The experimental studies of Nikuradse was used in order to model this parameter for channel flows, as follows:

$$L\left(\frac{y}{R}\right) = \frac{l_m}{R} = 0.14 - 0.08\left(\frac{y}{R}\right)^2 - 0.06\left(\frac{y}{R}\right)^4. \tag{20}$$

To further completeness of the model, Cebeci and Bradshaw added the Van Driest damping function:

$$L\left(\frac{y}{R}\right) = \frac{l_m}{R} = \left\{0.14 - 0.08\left(\frac{y}{R}\right)^2 - 0.06\left(\frac{y}{R}\right)^4\right\}\left\{1 - e^{[(\frac{y}{R}-1)\frac{Re_\tau}{A}]}\right\}, \tag{21}$$

with $A = 26$ as the Cebeci's constant. Thus, we had the mixing length defined by:

$$l_m = LR, \tag{22}$$

L being a function in the y axis, given by equation (21). So equation (18) can be rewritten as:

$$\frac{\partial}{\partial y}\left(\left(\alpha - \frac{L^2R^2}{Pr_t}\frac{\partial \overline{u}}{\partial y}\right)\frac{\partial \overline{T^*}}{\partial y}\right) = \overline{u}\frac{\partial\left(\overline{T_w}\right)}{\partial x}. \tag{23}$$

To compare the present work with literature models, this equation was nondimensionalized using the wall coordinates. It was considered: $\tilde{y} = \frac{y.Re_\tau}{R}$, $\tilde{\overline{u}} = \frac{\overline{u}}{u_\tau}$, $\tilde{\overline{T}} = \frac{\overline{T}}{T_\tau}$, $\tilde{\overline{T^*}} = \frac{\overline{T^*}}{T_\tau}$, $Re_\tau = \frac{u_\tau R}{\nu}$, $Pr_t = \frac{\nu_t}{\alpha_t}$, $Pr = \frac{\nu}{\alpha}$, $T_\tau = \frac{q_w}{\rho C_p u_\tau}$, $\frac{\partial(T_m)}{\partial x} = \frac{q_w}{u_m R \rho C_p}$ and $\frac{\partial \overline{p}}{\partial x} = -\frac{u_\tau^2 \rho}{R}$. What, substituting in (23) results in (24):

$$\frac{\partial}{\partial \tilde{y}}\left(\left(\frac{Re_\tau}{Pr} - \frac{L^2Re_\tau^3}{Pr_t}\frac{\partial \tilde{\overline{u}}}{\partial \tilde{y}}\right)\frac{\partial \tilde{\overline{T^*}}}{\partial \tilde{y}}\right) = \frac{\tilde{\overline{u}}}{\tilde{u_m}}. \tag{24}$$

It is important to note that there is the velocity in the equation (24), that is, for the development of the thermal problem, the development of the dynamic channel profile is necessary. For this, a previously established RANS methodology [13] was used, as follows:

$$\frac{\partial \tilde{\overline{u}}}{\partial \tilde{y}} = -\frac{2\tilde{y}\frac{1}{Re_\tau}}{1 + \sqrt{1 + 4L^2Re_\tau^2\tilde{y}}}. \tag{25}$$

In this way, there was the first derivative of velocity in an continuous form.

4 Numerical and algebraic models proposition

To discretize the differential equation, an Eulerian domain was used. For the velocity a fourth-order Runge-kutta method was applied, while the temperature was arranged in a central differences scheme that had to be solved implicitly. The dynamic model is solved first, and its numerical result are used in the solution of the thermal profile. The cell center was used in a such way that the wall was placed at the cell center, and a point between cells was placed in the center of the channel. The convergence of the numerical results is shown in figure 4:

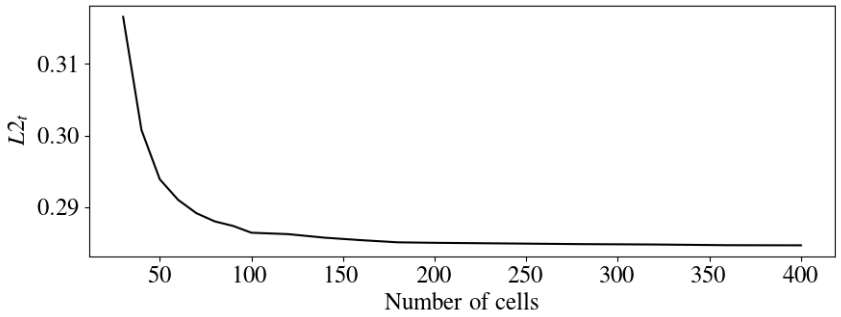

Figure 4: Norm L2 from thermal simulation and DNS up to 400 cells, with $Re_\tau = 1020$.

4.1 Preliminary results

Initially the turbulent Prandtl number, $Pr_t = 0.71$, was used as in the literature. The obtained results presented in figure 5 are compared with DNS from [9] and [10], using the norm L2.

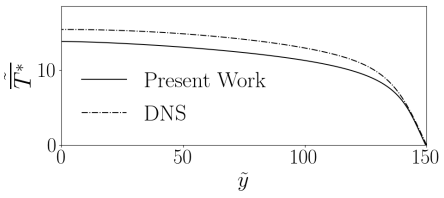

(a) $Re_\tau = 150$, $L2_t = 1.42$

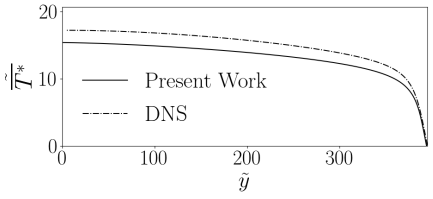

(b) $Re_\tau = 395$, $L2_t = 1.55$

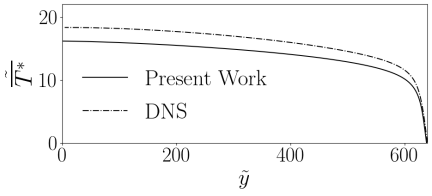

(c) $Re_\tau = 640$, $L2_t = 1.79$

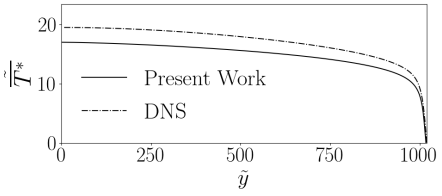

(d) $Re_\tau = 1020$, $L2_t = 2.04$

Figure 5: Temperature distribution for $Pr_t = 0.71$, $A = 26$ and $Pr = 0.71$

First results weren't satisfactory. It was noticed that the turbulent Prandtl number had great influence on the outcome, so the turbulent Prandtl number from [9] and [10] (figure 6) was used

as a parameter in the program, obtaining an L2 norm of 0.19 to $Re_t = 640$. Thus it was identified that the problem was in the parametrization of the turbulent Prandtl number and it became the focus of the present research.

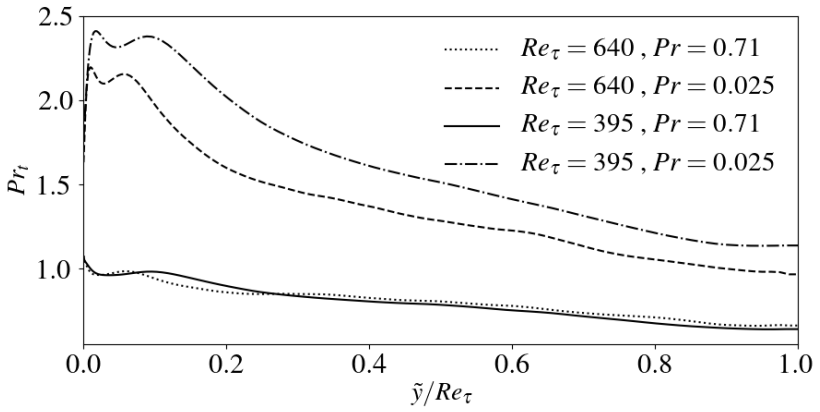

Figure 6: Turbulent prandtl number from DNS in function of $\tilde{y}/Re_\tau$ in the channel.

Thus, the effort to propose a parameterization adjusted for the turbulent Prandtl number started. In this sense it was tried to adjust a value for which the error was minimal, comparing to the DNS. In this regards, the differential evolution algorithm methodology was applied.

4.2 The meta-modeling, with the genetic algorithm: Differential Evolution (DE)

A differential evolution algorithm [14] that searched for a minimal parameter of interest for a given function was used. It was considered the turbulent Prandtl number as an editable variable and the smaller error as the aim pattern. The error was calculated comparing the resulting temperature with DNS data ([9] and [10]). It was obtained a turbulent Prandtl number of 0.9, for the Reynolds number $Re_\tau = 1020$.

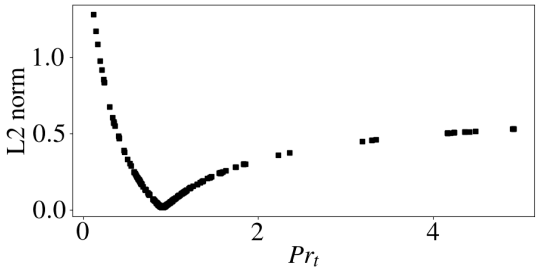

Figure 7: Genetic algorithm iterations, with simulations for $Re_\tau = 1020$. Convergence on $Pr_t = 0.9$.

The turbulent Prandtl number obtained, $Pr_t = 0.9$ which minimize the error on temperature field, was considered to the others Reynolds numbers, resulting on figure 8.

Although the results were much better as compared with figure 5, the model had to be further improved. The turbulent Prandtl number varies with the Reynolds number as observed on (fig.6),

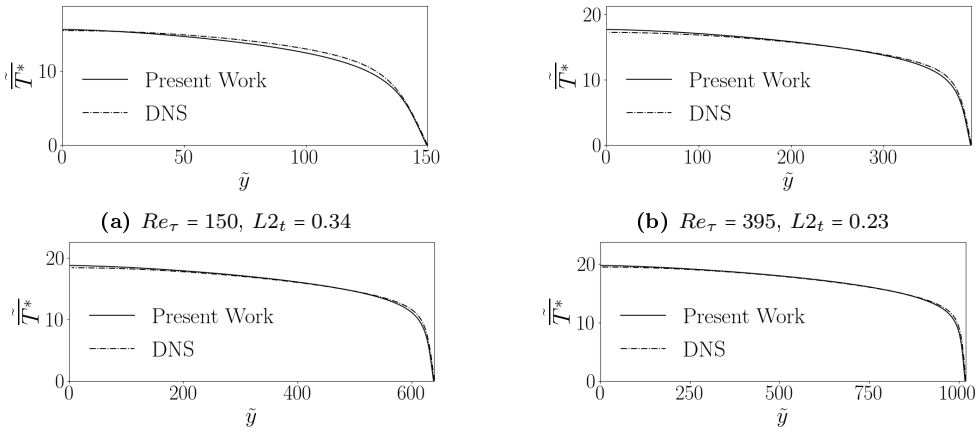

(a) $Re_\tau = 150$, $L2_t = 0.34$ **(b)** $Re_\tau = 395$, $L2_t = 0.23$

(c) for $Re_\tau = 640$, $L2_t = 0.19$ **(d)** for $Re_\tau = 1020$, $L2_t = 0.14$

Figure 8: Results of temperature simulations for $Pr_t = 0.9$, $A = 26$ and $Pr = 0.71$

so a model that contemplate this fact had to be proposed. In order to obtain a curve for Pr_t as a function of Re_τ, the same optimizing algorithm had to be used to determine an ideal turbulent Prandtl number for each Reynolds number available in the DNS data base [9] and [10]. The best turbulent Prandtl numbers obtained are summarized in table 1.

Table 1: Ideal turbulent Prandtl Numbers adjusted for each Reynolds number, with the Cebeci constant $A = 26$

Re_τ	Pr_t
150	0.94531
395	0.89531
640	0.89531
1020	0.90000

By performing a polynomial curve fit, a model adjusted for the turbulent Prandtl number as a function of the Reynolds number was developed:

$$Pr_t = -4.5604 * 10^{-10} Re_\tau^3 + 9.5690 * 10^{-7} Re_\tau^2 - 6.1715 * 10^{-4} Re_\tau + 1.0178. \quad (26)$$

The result of the simulations were much accurate, even more than the simulations with the turbulent Prandtl numbers set as the mean values of the ones from the DNS data (fig.6). These results can be seen in figure 9.

Other manners of reducing the inaccuracy were searched. The velocity profile was a possibility, as it plays an important role in the error of the method. Simulations were carried developing just this physical property, and there was error associated too (fig.10).

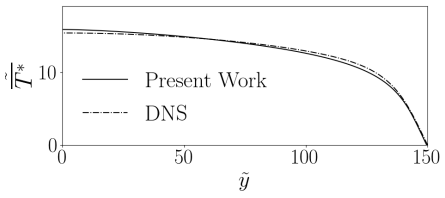

(a) $Re_\tau = 150$, $L2_t = 0.26$

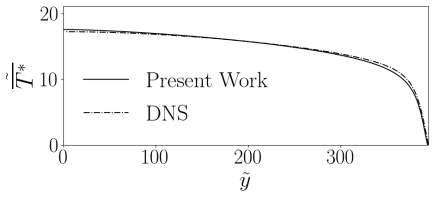

(b) $Re_\tau = 395$, $L2_t = 0.22$

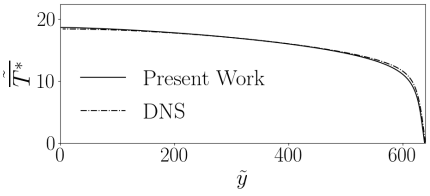

(c) $Re_\tau = 640$, $L2_t = 0.17$

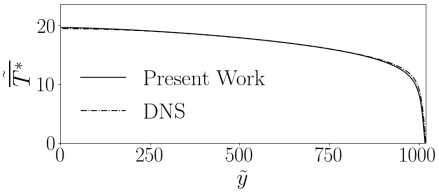

(d) $Re_\tau = 1020$, $L2_t = 0.14$

Figure 9: Results of temperature simulations for $Pr_\tau(Re_\tau)$, $A = 26$ and $Pr = 0.71$.

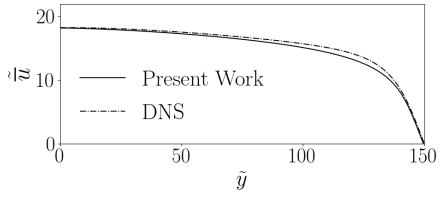

(a) $Re_\tau = 150$, $L2_d = 0.47$

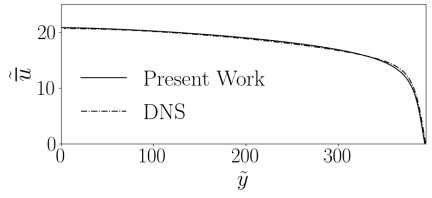

(b) $Re_\tau = 395$, $L2_d = 0.17$

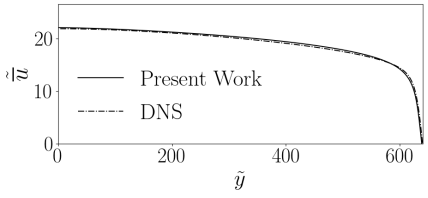

(c) $Re_\tau = 640$, $L2_d = 0.23$

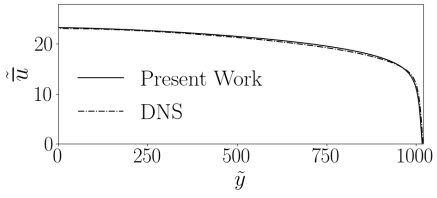

(d) $Re_\tau = 1020$, $L2_d = 0.23$

Figure 10: Results of velocity simulations for $A = 26$

A adjusted model was proposed in the present work for the Cebeci's constant A aiming to reduce it's error, and by extension, making the method more accurate. The same algorithm used to find the ideal turbulent Prandtl numbers was used to find an ideal Cebecis's constant for each Reynolds number. The velocity from DNS available was used to calculate de L2 norm. The Cebeci constant "A" was defined as an editable variable for the program, and the L2 norm was set as a parameter of interest. The results for ideal Cebeci's constants can be seen ahead.

From the resulting points of the optimization algorithm, a model was prepared and adjusted for a Cebeci function:

$$A\left(Re_\tau\right) = \frac{Re_\tau^{0.0451*\ln(Re_\tau)} * e^{5.2753}}{Re_\tau^{0.6094}}. \tag{27}$$

Then, it result in an adjusted method for the proposed Cebeci's function, optimized using minimal error relative to the velocity, as can be seen in the simulations, there was a improvement on the velocity calculation:

Table 2: Ideal Cebeci's constant adjusted for each Reynolds number

Re_τ	A
150	28.616180
395	25.673782
640	25.001266
1020	25.002136

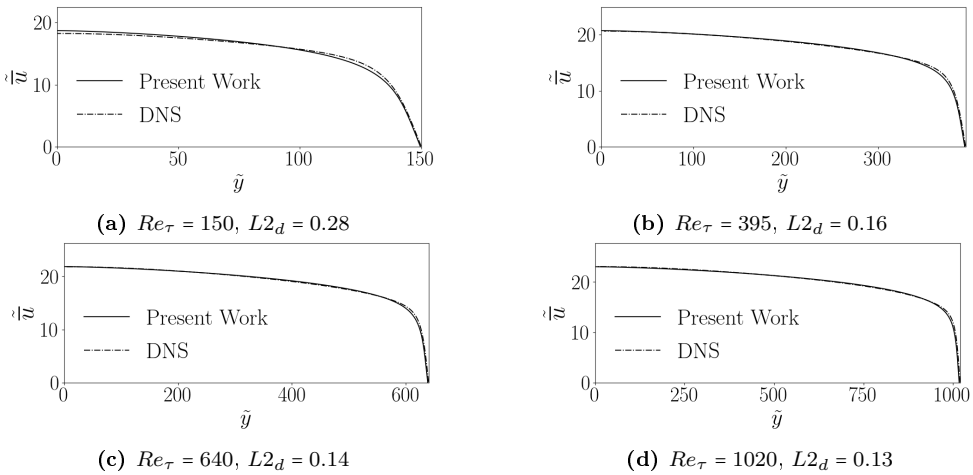

(a) $Re_\tau = 150$, $L2_d = 0.28$ **(b)** $Re_\tau = 395$, $L2_d = 0.16$

(c) $Re_\tau = 640$, $L2_d = 0.14$ **(d)** $Re_\tau = 1020$, $L2_d = 0.13$

Figure 11: Results in velocity distribution for A modeled.

With the Cebeci's function adjusted, a new group of optimizations were made, with the same differential evolution methodology, taking into consideration this new formulation for the Cebeci's constant. Such study resulted in a new set of optimal turbulent Prandtl number for each DNS sample Reynolds number, as follows:

Table 3: Ideal turbulent Prandtl Numbers adjusted for each Reynolds number, with the Cebeci's function modeled.

Re_τ	Pr_t
150	0.88594
395	0.90156
640	0.91094
1020	0.91406

A new model could be proposed for the Turbulent Prandtl number.

$$Pr_t = 4.5290 * 10^{-12} Re_\tau^3 - 5.7395 * 10^{-8} Re_\tau^2 + 9.397 * 10^{-5} Re_\tau + 0.8731. \tag{28}$$

With such parametrization, a new set of simulations were made, with the following results:

The Cebeci's values that resulted in a minor error for the velocity don't had the same effect on the temperature results. The Cebeci was modeled for the minimum velocity error, not being the best for the thermal solution. Algebraically, the Cebeci's function appears two times as seen in equations 24 and 25. Then, it is possible to propose two Cebeci's function models. One for the dynamical simulation A_d, and one for the temperature simulations A_t.

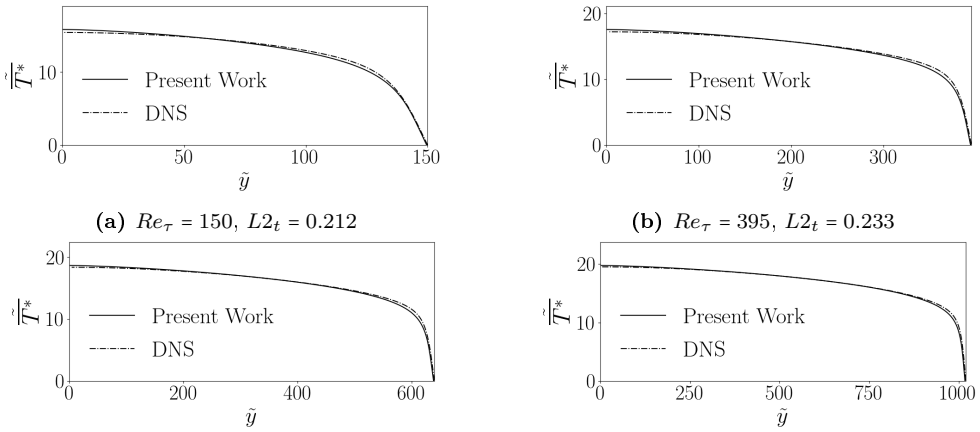

(a) $Re_\tau = 150$, $L2_t = 0.212$ **(b)** $Re_\tau = 395$, $L2_t = 0.233$

(c) $Re_\tau = 640$, $L2_t = 0.205$ **(d)** $Re_\tau = 1020$, $L2_t = 0.175$

Figure 12: Results of temperature simulations for $Pr_\tau(Re\tau)$, $A(Re_\tau)$ and $Pr = 0.71$

Another method of adjustment on differential evolution is the multi objective adjustment. Such approach was used to consider more then one variable simultaneously for optimization. This method was used to adjust the thermal Cebeci's function and the Turbulent Prandtl number for the minor error (L2 norm) in the resulting temperature field for each DNS sample. The Cebeci function for velocity was considered in the previously development. New ideal values were found for the turbulent Prandtl number and the thermal Cebeci's constant:

Table 4: Ideal turbulent Prandtl Numbers and thermal Cebeci's function (A_t) adjusted for each turbulent Reynolds number, with the multi objective approach. The Cebeci for velocity (A_d) continued the same from table 2.

Re_τ	Pr_t	A_t	A_d
150	0.72530	37.25510	28.616180
395	0.76821	34.24176	25.673782
640	0.81896	31.27627	25.001266
1020	0.86179	28.73726	25.002136

With such numerical DATA, new models were both proposed for the Turbulent Prandtl number and the thermal Cebeci's function:

$$A_t = \frac{Re_\tau^{0.0395\ln(Re_\tau)^2 - 0.7588\ln(Re_\tau) + 4.6637}}{e^{5.6703}}, \tag{29}$$

$$Pr_t = -2.4892 * 10^{-10} Re_\tau^3 + 3.6036 * 10^{-7} Re_\tau^2 + 3.7921 * 10^{-5} Re_\tau + 0.7123. \tag{30}$$

More simulations were developed using such new proposed models.

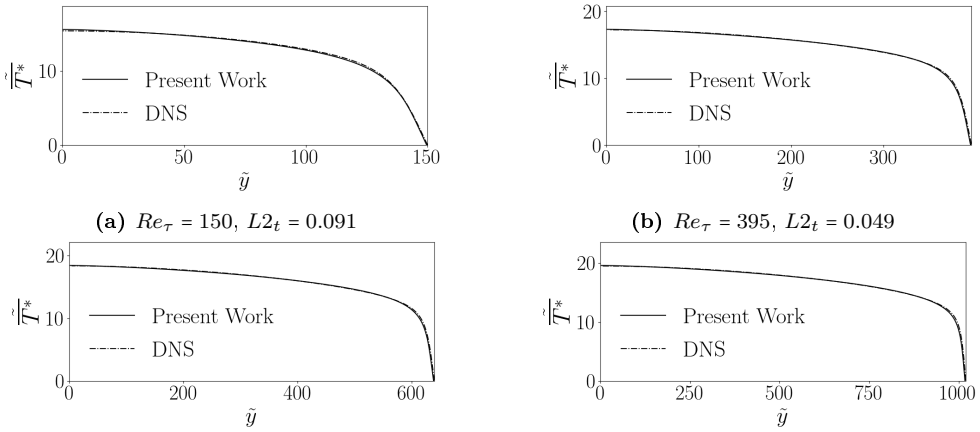

(a) Re_τ = 150, $L2_t$ = 0.091 **(b)** Re_τ = 395, $L2_t$ = 0.049

(c) Re_τ = 640, $L2_t$ = 0.061 **(d)** Re_τ = 1020, $L2_t$ = 0.076

Figure 13: Results of temperature simulations for $Pr_\tau(Re_\tau)$, $A_d(Re_\tau)$, $A_t(Re_\tau)$ and Pr = 0.71, with multi-objective adjustment.

5 Results

With such methods, it was studied the advantages and disadvantages of each one. A comparison between errors can be seen ahead, in figure 14:

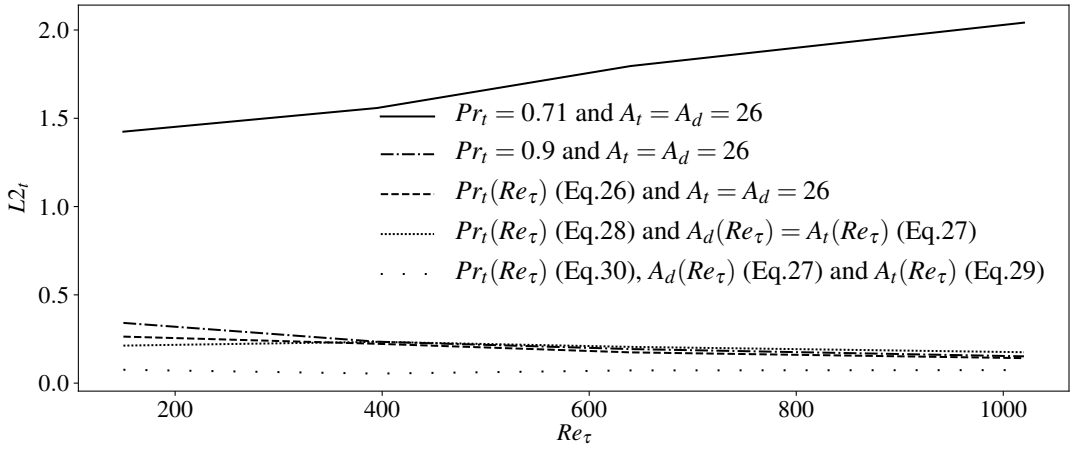

Figure 14: Comparison between all proposed models for Pr_t, A_d and A_v, in respect to the temperature results in comparison with DNS.

All the models developed on the present paper shown better results then the classical parametrization of Pr_t = 0.71 and A = 26 on the turbulent Poiseuille flow. The correction in the Cebeci's constant, although represented a smaller error in the velocity, didn't resulted in smaller errors in the temperature profile for all the domain. The model that presents the best results was the developed with the multi-objective differential evolution algorithm in with it was considered two Cebeci's functions for each domain (thermal and dynamical).

The dynamical Cebeci's constant optimization also caused gains in the velocity field in terms of velocity error, as seen in figure 15.

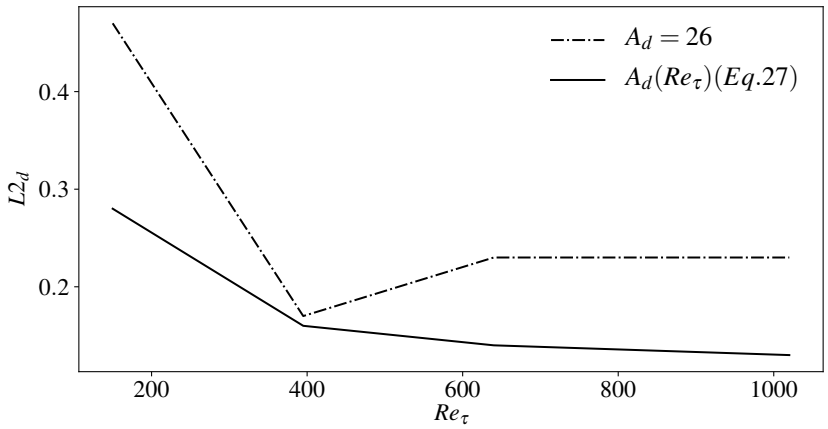

Figure 15: Comparison between the proposed models for A_d, in respect to the velocity results in comparison with DNS.

6 Conclusion

In the present paper it was successfully developed a semi-analytical methodology to calculate the temperature profile inside a channel with the Prandtl mixing length model, a classic closure model in the study of turbulence. The validations with DNS were satisfactory. Its is important to notice that such values of turbulent Prandtl number and Cebeci's function were applied for this particular case, as the parametrizations result from particular computational adjustments and simplifications of the physical abstractions that each model represents were assured. But they suited well for this case, resulting in accuracy and efficiency. The semi analytical method was successful in model the problem, as good results were obtained when used the turbulent Prandtl numbers from the DNS and the Cebeci function from literature. As for the models proposed, it is an idea to test then in other problems, with other geometries and using other kinds of turbulence closure models, as a way of testing their usability for other more complex flows problems.

7 Acknowledgments

It's opportune to thanks all the institutions involved with the viabilization of the present research project. The laboratory of fluids mechanic (MFLab) of the Mechanical Engineering College (FEMEC) of the Federal University of Uberlandia (UFU). PETROBRAS, CNPq, CAPES and FAPEMIG that contributed financially to this project.

References

[1] Basim O. and Hasan Turbulent Prandtl Number and its Use in Prediction of Heat Transfer Coefficient for liquids. Nahrain University, College of engineering Journal (NUCEJ) Vol.10, No.1 2007.

[2] John C. S., Edward O. and Tamas T., Modeling Two-Dimensional Fluid Flows with Chaos Theory, Johns Hopkins APL Technical Digest, volume 18, number 2, 193-202, 1997.

[3] Prandtl L., Uber die ausgebildete Turbulenz, ZAMM, 1925.

[4] Cebeci T. and Bradshaw P., Physical and computational aspects of convective heat transfer, Springer, New York, 1984.

[5] Neto A. S., Turbulência nos fluidos, textbook of the post graduate mechanical engineering course of federal university of Uberlândia, Uberlândia, Brazil, 2018.

[6] Kawamura, H. , Abe, H. and Shingai, k. , DNS of turbulence and heat transport in a channel flow with different Reynolds and Prandtl numbers and boundary conditions., Turbulence, Heat and Mass Transfer 3, (Proc. of the 3rd International Symposium on Turbulence, Heat and Mass Transfer), 2000.

[7] Kawamura H., Abe H. and Yuichi M., DNS of turbulent heat transfer in channel flow with respect to Reynolds and Prandtl number effects, Elsevier, Tokio, Japan, 1999.

[8] Poiseuille J. L. M., Recherches experimentales sur Ie mouvement des liquides dans les tubes de tres-petits diametres, Memoires presentes par divers savants a l'Academie Royale des Sciences de l'Institut de France, IX: 433-544, 1846.

[9] Kawamura H., Direct Numerical Simulation Data Base for Turbulent Channel Flow with Heat Transfer., <http://www.rs.tus.ac.jp/ t2lab/db/index.html>, Laboratory of Thermo-fluid dynamics, Department of Mechanical Engineering, Faculty of Science and Technology, Tokyo University of Science, Noda-shi, Chiba-ken, Japan, 2007.

[10] Kasagi H., Horiuti K., Miyake Y., Miyauchi T. and Nagano Y., Establishment of the Direct Numerical Simulation Data Bases of Turbulent Transport Phenomena, <http://thtlab.jp/DNS/dns_database.html>, Co-operative Research No. 02302043, Bunkyo-ku, Tokyo 113 , 1992.

[11] Cengel Y. A. and Cimbala J. M., Fluid mechanics Fundamentals and Applications, First edition, McGraw-Hill series in mechanical engineering, 2006.

[12] Incropera, Freank, P., Dewitt, David, P., *fundamentals of Heat and Mass Transfer*, 3rd edition, p. 310-316, 2007, LTC, (INCROPERA and DEWITT).

[13] Antonialli L. A. and Silveira A. N., Theoretical study of fully develop turbulent flow in a flat channel, using prandtl's mixing length model, 2015.

[14] Price K. V., Storn M. R. and Lampinen A. J., Differential Evolution, a practical approach to Global Optimization, 2005.